

**EMPLACEMENT OF LAYERED CRATER EJECTA ON MARS.** S. M. Baloga<sup>1</sup>, S. A. Fagents<sup>2</sup>, and L.S. Glaze<sup>3</sup>,  
<sup>1</sup>Proxemy Research (20528 Farcroft Lane, Gaithersburg, MD 20882, ([steve@proxemy.com](mailto:steve@proxemy.com)) <sup>2</sup>Univ. Hawaii at Manoa, Honolulu, HI 96822, ([fagents@hawaii.edu](mailto:fagents@hawaii.edu)), <sup>3</sup>NASA's Goddard Space Flight Center (Code 698, Greenbelt, MD 20771, [Lori.S.Glaze@nasa.gov](mailto:Lori.S.Glaze@nasa.gov))

**Introduction:** Layered ejecta deposits of impact craters on Mars take three main morphological classifications: single-layer (SLE), multi-layer (MLE) and double-layer (DLE) ejecta deposits [1,2]. It has long been thought that these deposits involved a fluidizing agent, although it remains unclear whether the agent was vapor or liquid, or whether its origin was crustal or atmospheric [3,4,5]. However, morphologic studies continue to suggest emplacement of the layered deposits as ground-hugging flows [6,7,8]. A model of a ground-hugging flow of ejecta has been formulated to answer the following questions: Why are there 3 different morphologies? What are the quantitative parameters of emplacement, such as flow velocity and runout duration? What can be inferred about the fluidizing agent? Why does the complexity of the outer margins and interior morphologies increase with crater diameter? What distinguishes DLE emplacement?

**The Model:** A basic mathematical model for ground-hugging flow was developed and solved to describe the time-dependent advance of the ejecta flow. The model is based on the conservation of ejecta mass, volume and momentum. It uses a 'shallow-wave' form common in numerous applications to catastrophic terrestrial and planetary mass flows. Of particular interest is a basal friction term described by a parameter  $C$ , which has been documented for many different types of mass flows on Earth (e.g., floods, lahars, debris) for comparison [9,10].

For Mars parameters, the model shows that the ejecta flow is comprised of two advancing waves. The ways in which these waves propagate and interact provide a broad unifying explanation for the issues identified above. Figure 1 is a cartoon of the flow model for the ground-hugging flow, emphasizing the dual wave nature of the flow and some of the mathematical complexity in obtaining solutions for the time-dependent depth ( $h$ ) and flow velocity ( $u$ ).

**Approach:** Planform lobateness [11, 12] was computed using THEMIS data for 35 fresh, relatively symmetric impact crater deposits on Lunae Planum and for the craters Bacolor in Utopia Planitia [13] and Tooting in Amazonis Planitia [14].

The Lunae Planum craters were classified as either single layer (SLE) or multilayer (MLE). Crater diameters range from 4-17 km. Bacolor is a 19 km diameter crater with a typical double layer ejecta (DLE) deposit, while Tooting is a 36 km diameter MLE featuring a

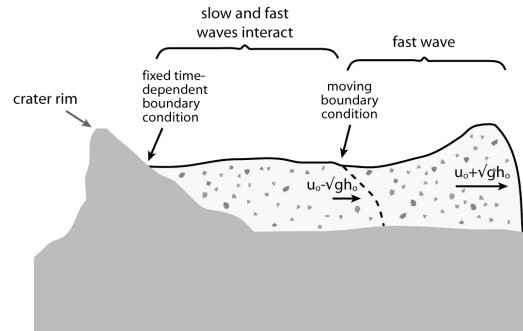


**Fig. 1.** Ground-hugging ejecta flow model

highly complex, multi-lobed deposit. The lobateness of these craters has a remarkably strong positive correlation with crater diameter. Both THEMIS and overlapping HiRISE, CTX and HRSC images support an increase in the morphologic complexity of the deposit surfaces with crater diameter.

For 27 of the Lunae Planum craters, Bacolor, and Tooting, it is possible to estimate the average rampart height and the leading and trailing slopes using the gridded MOLA data. Craters were included in the population only if at least two MOLA transects could be used to discern the maximum height and leading and trailing slopes of the ramparts. In many cases, between 10 and 15 transect segments could be used. Remarkably, the average leading and trailing slopes of the ramparts of the Lunae Planum craters form a single statistical population that is independent of crater diameter. Both Bacolor and Tooting fall well within the limits of this population. This suggests that the terminal radial gradient of layered ejecta blanket topography is controlled by the material properties of the ejecta, rather than by some measure of the impact energy.

Progressively more complicated solutions of the mathematical shallow-wave model of the ground-hugging were found and matched to the rampart shape data for each crater in Lunae Planum. The simplest 'basal glide' case features no friction between the ground-hugging flow and the pre-existing surface. Typical model profiles of the flow thickness are shown in Figure 2 for three different times. The steepness of the leading wave was adjusted to match the trailing slopes of the Lunae Planum craters. This matching process provides immediate, albeit rough, quantitative constraints on the emplacement parameters.

Representative results for the Lunae Planum craters are shown in Table 1 ( $R/O$ =runout,  $h_0$ =initial flow depth,  $u_0$ =initial flow velocity,  $T$ =emplacement time).

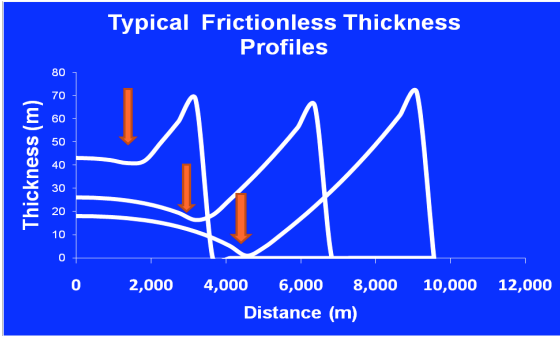


Fig. 2. Theoretical profiles from shallow-wave model

Table 1.

|         | SLE-1 | SLE-2 | SLE-3 | MLE-1 | MLE-2 |
|---------|-------|-------|-------|-------|-------|
| Diam km | 14    | 10    | 7     | 12    | 10    |
| R/O km  | 9     | 6     | 7     | 10    | 7     |
| ho m    | 71    | 56    | 61    | 91    | 93    |
| uo m/s  | 91    | 42    | 29    | 97    | 69    |
| Ts      | 85    | 111   | 150   | 83    | 60    |

All inferred emplacement parameters, particularly the flow velocities, appear to be reasonable and consistent with catastrophic terrestrial mass flows.

The shallow-wave model has intrinsic instabilities for various sets of parameters. It appears likely that these instabilities cause the transition from a flow that produces an SLE deposit to one that produces an MLE. This hypothesis was investigated for Tooting crater (Fig. 3.). Assuming the instability was triggered somewhere between 10 and 20 km from the rim, emplacement parameters similar to those in Table 1 were found. The emplacement parameters for Tooting were not significantly different from the Lunae Planum results, except for the emplacement time and the duration of supply to the flow. For Tooting, the transit time and supply duration are about 4-6 times longer than the average of the Lunae Planum SLE cases.

The shallow wave model was also solved with basal friction in the leading wave. The leading slope of the flow is controlled by the friction parameter  $C$ . Terrestrial experience shows that  $C$  varies from 0.0025 for turbulent water flow to approximately unity for dense debris flows [9,10]. The model flow depth profiles were matched to the leading slope data for four SLE deposits in Lunae Planum. The resulting inferred  $C$  values range from 0.001 to 0.003. This suggests the frictionless basal glide results are indeed reasonable first-order estimates. Because the deposits are particulates, the results further imply that vapor rather than liquid water must have been the fluidizing agent.

When typical terrestrial  $C$  values are used in the model, the faster moving wave slows dramatically over a few kilometers. The trailing wave component can

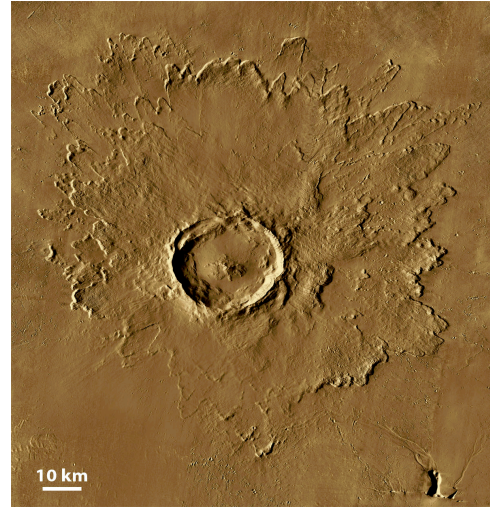


Fig. 3. Tooting Crater

then override the leading one, as has been documented for terrestrial debris flows. This process provides a direct explanation for the emplacement of the DLE deposits recently elaborated in [13].

**Conclusions:** The topographic shapes of the ramparts in layered ejecta provide critical new information that permits modeling and new inferences about ground-hugging ejecta flows on Mars. The shallow wave model provides a unifying interpretation for the formation of SLE, DLE, and MLE deposits. An MLE deposit, instead of an SLE deposit, forms when the flow is fed for a longer time and instability is promoted. The inherent instability also supports the quantitative increase in lobateness and morphologic complexity with increasing crater diameter. Preliminary applications of the model to SLE craters in Lunae Planum suggest that the fluidizing agent was vapor instead of liquid water. Although the mechanism has not yet been isolated, the shallow-wave model can also explain the formation of the seemingly distinct DLE deposits.

**References:** [1] Barlow, N.G. et al. (2000), *JGR*, 105(E11), 26,733-738. [2] Garvin, J.B. et al. (2000), *Icarus*, 144, 329-352. [3] Carr, M.H. et al. (1977), *JGR*, 82, 4055-65. [4] Barnouin-Jha, O.S. and P. Schultz (1998), *JGR*, 103, 25,739-756. [5] Barlow, N.G. and C.B. Perez, (2003), *JGR*, 108(E8), 5085, doi:10.1029/2002JE002036. [6] Baloga, S.M. et al. (2005), *JGR*, 110, E10001, doi:10.1029/2004JE002338. [7] Barnouin-Jha, O.S. et al. (2005), *JGR*, 110, E04010, doi:10.1029/2003JE002214. [8] Mouginis-Mark, P.J., and S.M. Baloga (2006), *Meteor. Planet. Sci.*, 41, 1469-1482. [9] Bulmer, M.H. et al. (2002), *JGR*, 107, doi:10.1029/2001JE001531. [10] Baloga, S.M. et al. (1995), *JGR*, 100(B12), 24,509-519. [11] Kargel, J.S. (1986), *Lunar Planet. Sci XVII*, 410-411 (abs.). [12] Barlow, N.G. (1994), *JGR*, 99(E5), 10,927-935. [13] Boyce, J.M. and P.J. Mouginis-Mark (2006), *JGR*, 111, doi:10.1029/2005JE002638. [14] Mouginis-Mark, P.J. and H. Garbeil (2007), *Meteor. Planet. Sci.*, 42, 1615-26.